polarized parallel to it (B_2). This identification of the eigenvectors may prove helpful in unravelling the vibrational couplings that determine the frequencies and isotope shifts of the bands.

Conclusions

(1) ^{54}Fe isotope shifts lead to definitive assignments of the ν_3 asymmetric stretching vibration of the FeS_4 tetrahedron, which is split into components at 376, 363, and 348 cm^{-1}. The lower than expected isotope shifts for the latter two established that they are coupled to protein vibrational modes, probably involving SCC bending in the cysteine ligands. The 324-cm^{-1} shoulder on the 314-cm^{-1} ν_1 band is tentatively assigned to a δ_{SCC} band.

(2) Variable-excitation and depolarization measurements provide assignments for the A_1 and E components of the ν_2 and ν_4 modes; the latter can mix the B_2 and E components of the lower energy ($S_\pi \rightarrow Fe_{d\pi}$) charge-transfer transition. A similar enhancement pattern identifies the lower two ν_3 bands, at 363 and 348 cm^{-1}, with the perpendicular (E) components of the asymmetric stretch.

(3) Numerous overtone and combination bands are observed in the frozen-solution spectra, with normal intensity patterns. A band at 653 cm^{-1} is assigned to S–C stretching of the cysteine ligand.

The assignments are detailed in Table I.

Acknowledgment. This work was supported by NIH Grant GM 13498.

Registry No. ^{54}Fe, 13982-24-6; ^{56}Fe, 14093-02-8.

Contribution from the Department of Applied Chemistry, Faculty of Engineering, Yamanashi University, Takeda, Kofu 400, Japan, and Electrotechnical Laboratory, Sakura-mura, Niihari-gun, Ibaraki 305, Japan

EXAFS Study of Chromium Ions in the Mixed-Solvent System of Formamide and Ammonium Formate

Michihiro Miyake,*[†] Nobuhiro Nakagawa,[†§] Hiroyuki Ohyanagi,[‡] and Takashi Suzuki[†]

Received February 20, 1985

EXAFS (extended X-ray absorption fine structure) spectra of Cr ions exhibiting two oxidation states, Cr(VI) and Cr(III), in the mixed-solvent system of $HCONH_2$ and $HCOONH_4$ have been investigated for the Cr K edge by Fourier transform and parameter-fitting methods. In the mixed-solvent system, it was found that Cr(VI) ions form mononuclear CrO_4^{2-} tetrahedra with Cr–O bond lengths of 1.61 Å and Cr(III) ions form mononuclear $[Cr(HCOO)_x(HCONH_2)_y]^{3-x}$ ($x + y = 6$; $4 \le x \le 6$) octahedra with Cr–O bond lengths of 2.00 Å. The CrO_4^{2-} tetrahedra, which exist in the mixed-solvent system at an initial state of dissolution of CrO_3, are transformed into the $[Cr(HCOO)_x(HCONH_2)_y]^{3-x}$ octahedra by heating reduction.

Introduction

Ammonium formate ($HCOONH_4$), which has been found to be a molten salt with low melting point (mp 116 °C),[1] is partially decomposed into formamide ($HCONH_2$) and water although molten $HCOONH_4$ can dissolve various metallic oxides that are insoluble in water. The mixed-solvent system of $HCONH_2$ and $HCOONH_4$, therefore, has been utilized as the model solvent of the molten $HCOONH_4$ bath. The dissolution characteristics of metallic oxides in the $HCONH_2$ + $HCOONH_4$ system have been investigated on the basis of visible absorption spectra and ESR spectra, and this mixed-solvent system was found to have outstanding properties as a metal-plating bath.[1-4] Though the structure of liquid $HCONH_2$ was analyzed by X-ray diffraction,[5,6] the coordination structure of metallic ions in the $HCONH_2$ + $HCOONH_4$ system has been unexplained.

The Cr atoms exhibit two oxidation states, Cr(VI) and Cr(III), in the $HCONH_2$ + $HCOONH_4$ system, and a blackish corrosion-resistant chromium film can be successfully electrodeposited on the condition that there exist Cr(III) ions in this bath.[2] It is of interest to compare the coordination structure of Cr(III) ions with that of Cr(VI) ions in the $HCONH_2$ + $HCOONH_4$ system to aid in elucidating the mechanism of electrodeposition from this bath.

In this paper, we describe the results obtained by EXAFS (extended X-ray absorption fine structure) experiments of Cr(VI) and Cr(III) ions in the $HCONH_2$ + $HCOONH_4$ system for the Cr K edge. The coordination structures of the Cr(VI) and Cr(III) ions are demonstrated on the basis of the experimental results, associated with previous results.[1,2]

Experimental Section

Sample I, which was a brown solution, was prepared by dissolving 3.2 g (0.03 mol) of CrO_3 and 25 g (0.4 mol) of $HCOONH_4$ in 100 cm^3 of $HCONH_2$ at room temperature. Sample II, which was a purple solution, was prepared by reducing sample I with stirring at about 90 °C for 36 h. The visible absorption spectra of these solutions were measured to clarify the oxidation state of the Cr ions.

The solution was contained in an aluminum cell with Kapton (30 μm) windows through which X-rays were passed, and the thickness of the cell was adjusted in order to get the optimum absorption jump at the Cr K edge. Reference compounds such as K_2CrO_4 and Cr_2O_3 crystals were chosen, considering the oxidation states of the Cr ions in the solutions. Cr(VI) ions are tetrahedrally surrounded by four O atoms in the K_2CrO_4 crystal belonging to K_2SO_4 type, and Cr(III) ions are octahedrally surrounded by six O atoms in Cr_2O_3 crystals belonging to corundum type. Crystals were ground into fine powders and sandwiched between adhesive tapes. Special care was taken to produce homogeneous films to avoid distortion in the spectra.

The X-ray absorption spectra have been measured on the EXAFS apparatus[7,8] installed at BL 10B in the Photon Factory of the National Laboratory for High Energy Physics (KEK). The synchrotron radiation, running typically at 2.5 GeV with the beam current in the range 70–150 mA, was monochromated with a silicon (311) channel-cut crystal under helium gas. Intensities were monitored by two ionization chambers (I_0 and I) filled with N_2 and Ar gases, respectively. The spectral range covered was 1300 eV, of which 300 eV was preedge, and an energy resolution of 1.7 eV with a photon flux of 10^8–10^9 photons/s was achieved in the vicinity of the Cr K edge (5.989 keV).

Results and Discussion

The visible absorption spectra for solutions I and II are shown in Figure 1. The maxima at about 410 nm for solution I and

---

[†] Yamanashi University.

[‡] Electrotechnical Laboratory.

[§] Present address: Shin-etsu Chemical Co., Gunma, Japan.

(1) Suzuki, T.; Hayakawa, Y. *Molten Salts* **1976**, *19*, 127.
(2) Suzuki, T.; Hatsushika, T.; Hayakawa, Y. *Molten Salts* **1980**, *23*, 135.
(3) Suzuki, T.; Hatsushika, T.; Hayakawa, Y. *Nippon Kagaku Kaishi* **1982**, 1017.
(4) Hayakawa, Y.; Hatsushika, T.; Suzuki, T. *Denki Kagaku oyobi Kagyo Butsuri Kagaku* **1983**, *51*, 203.
(5) Ohtaki, H.; Funaki, A.; Rode, B. M.; Reibnegger, G. J. *Bull. Chem. Soc. Jpn.* **1983**, *56*, 2116.
(6) Miyake, M.; Kaji, O.; Nakagawa, N.; Suzuki, T. *J. Chem. Soc., Faraday Trans. 2* **1985**, *81*, 277.
(7) Photon Factory Activity Report of the National Laboratory for High Energy Physics, Japan, 1982/1983; V-28.
(8) Ohyanagi, H.; Matsushita, T. *Kotai Butsuri* **1983**, *18*, 515.

0020-1669/86/1325-0700$01.50/0

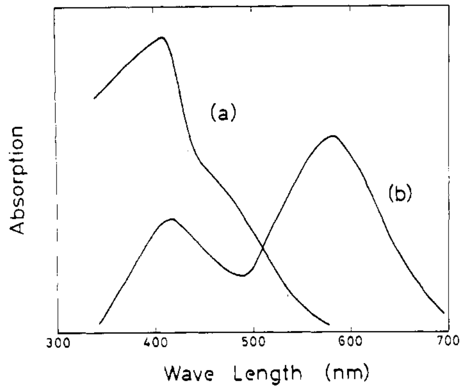

Figure 1. Visible absorption spectra of (a) solution I and (b) solution II.

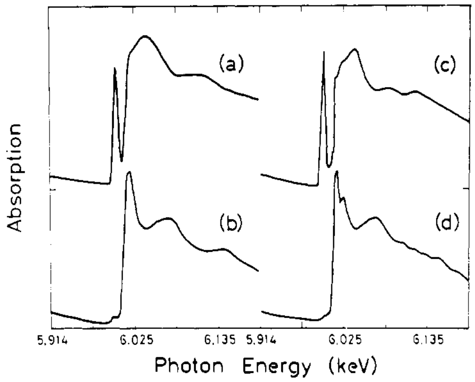

Figure 2. Near-edge structures of materials containing the Cr ions on the Cr K edge: (a) solution I; (b) solution II; (c) K_2CrO_4; (d) Cr_2O_3.

at about 420 and 580 nm for solution II were observed. By comparison with previous results[2], the existence of Cr(VI) and Cr(III) ions in solutions I and II was anticipated, respectively.

The near-edge structures for solutions I and II and for K_2CrO_4 and Cr_2O_3 on the Cr K edge are shown in Figure 2. A sharp peak before the absorption edge was observed in Figure 2a, while the peak decreases its intensity and is barely discernible in Figure 2b. This peak was found in the reference compounds, and the near-edge structures for solutions I and II are similar to those for K_2CrO_4 and Cr_2O_3, respectively. From the comparison between the solutions and reference compounds, the decrease of the intensity of the peak was assigned as corresponding to the transition of the density state of the electrons, namely, Cr(VI) → Cr(III) and the loss of tetrahedral symmetry.

The EXAFS oscillations $\chi(k)$ were extracted from the raw absorption spectra by the following procedures. The preedge, from 300 eV below the edge to the edge, was first approximated by eq 1, extrapolated above the edge, and subtracted from the whole

$$f(E) = \alpha E^{\beta} + \gamma \quad (1)$$

spectrum. In eq 1 E is the energy of the photoelectrons and α, β, and γ are parameters to be determined by the least-squares calculation.[8] Second, the atomic contribution to the absorption spectra was subtracted by using either a polynomial fit or a cubic splain fit to the highest energy possible. The final result was obtained by removing the long-wavelength oscillations by Fourier filtering. The extracted EXAFS spectra are shown in Figure 3. In the single scattering approximation, the extracted EXAFS[9,10] is described by eq 2, where N_i is the number of atoms of type i

$$\chi(k) = \sum_{i} k^{-1} N_i [A_i(k)] r_i^{-2} e^{-2r_i/\lambda} \sin(2kr_i + \phi_i(k)) e^{-2\sigma_i^2 k^2} \quad (2)$$

at a distance r_i from the absorption atom, σ_i the Debye–Waller type factor, and λ the mean free path of photoelectrons. $\phi_i(k)$ and $A_i(k)$ are the total phase shift and the back-scattering amplitude, respectively. k is the wavenumber of photoelectrons converted by eq 3, where E_0 is the zero energy of photoelectrons

$$k = [2m(E - E_0)/\hbar^2]^{1/2} \quad (3)$$

and is unknown in many cases. The position of the absorption edge was chosen as the value of E_0 at the first approach although this leads to errors in the estimation of the true bond length. This parameter in our investigations was regulated by the method mentioned later.

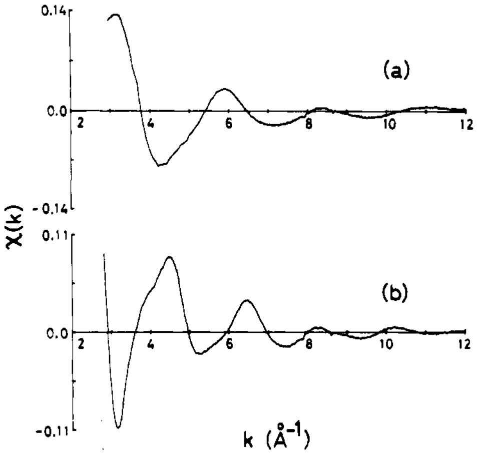

Figure 3. Extracted EXAFS spectra $\chi(k)$ for (a) solution I and (b) solution II.

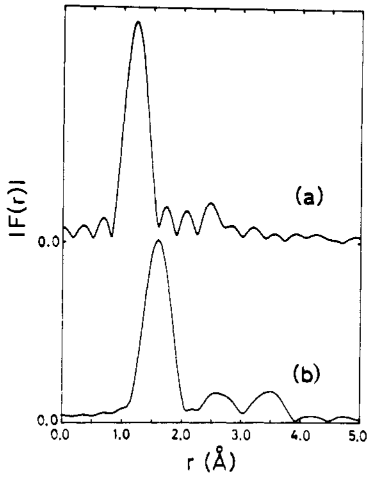

Figure 4. Magnitudes of Fourier transform $|F(r)|$ of $k^3\chi(k)$ curves for (a) solution I and (b) solution II.

The k^3-weighted $\chi(k)$ curves in the range $k = 3.5–12.0$ Å^{-1} were Fourier transformed to real space by using a Gaussian window function[11] to diminish a truncation effect. The magnitudes of the Fourier transform $|F(r)|$ for solutions I and II are shown in Figure 4. By comparison with the $|F(r)|$ curves for the reference compounds, the first prominent peaks, at 1.22 Å for solution I and at 1.58 Å for solution II, on the $|F(r)|$ curves were assigned to the O atoms tetrahedrally and octahedrally surrounding the central Cr ions, respectively. In the present structural analyses, the Cr ions were assumed to be coordinated to the O atoms. The reason for this assumption will be discussed later. No peak corresponding to the Cr···Cr interatomic distance could be found on the $|F(r)|$ curves for solutions I and II. This suggests that the Cr ions form mononuclear complexes in these solutions.

As the peaks on the $|F(r)|$ curve are shifted by the phase shifts of the absorbing and scattering atoms, the true bond length cannot be obtained from the $|F(r)|$ curves. The following two analytical procedures, therefore, were carried out in order to determine the true bond length, using the experimental Cr K edge absorption

---

(9) Sayers, D. E.; Stern, E. A.; Lytle, F. W. *Phys. Rev. Lett.* **1971**, *27*, 1204.
(10) Stern, E. A.; Sayers, D. E.; Lytle, F. W. *Phys. Rev. B: Solid State* **1975**, *11*, 4836.
(11) Lee, P. A.; Beni, G. *Phys. Rev. B: Solid State* **1977**, *15*, 2862.

Table I. Results of Parameter Fitting by Least-Squares Calculation for Solutions I and II and Zero Energy of Photoelectrons[a]

specimen	N	r, Å	σ, Å	R factor	E_0, keV
K_2CrO_4	4.0	1.636[17] 1.651 1.643 (2×)	0.060	0.126	5.998
Cr_2O_3	6.0	1.962 (3×)[18] 2.013 (3×)	0.067	0.085	5.996
soln I[b]	3.7	1.613	0.071	0.132	5.995
soln I[c]	3.8	1.617	0.069	0.120	5.995
soln II[b]	5.8	2.000	0.077	0.156	5.998
soln II[c]	5.9	2.003	0.076	0.141	5.998

[a] N = coordination number; r = bond length; σ = Debye–Waller type factor; R factor calculated by $R = \sum||k^3\chi(k)_{\text{obsd}}| - |k^3\chi(k)_{\text{calcd}}||/\sum|k^3\chi(k)_{\text{obsd}}|$ at intervals of 0.02 $Å^{-1}$ in the range from k = 4.0 to 11.0 $Å^{-1}$. Errors in least-squares calculation: ΔN, $\simeq 0.2$; Δr, $\simeq 0.007$; $\Delta\sigma$, $\simeq 0.003$. [b] Data are based on the K-absorption spectrum of the K_2CrO_4 crystal. [c] Data are based on the K-absorption spectrum of the Cr_2O_3 crystal.

spectra of the reference compounds. One is the method proposed by Martens et al.[12] and Rabe et al.[13] and the other the curve-fitting method by least-squares calculation.[14,15] The former was utilized to determine the value of E_0 and the latter to decide the coordination number, bond length, and Debye–Waller type factor. It was necessary to determine the value of E_0 in order to reduce errors in the estimation of the bond length.

The function $\psi(k)$ $(=2kr + \phi(k))$ was calculated from the back Fourier transform of the first shell on the $|F(r)|$ curve for each specimen. According to the transferability,[16] $\phi(k)_{\text{known}}$ was assumed to be equal to $\phi(k)_{\text{unknown}}$ in eq 2. Then, the difference between the Cr–O bond lengths in the solution and reference compound was calculated from eq 4. The value of E_0 was varied

$$\Delta r(k) = [\psi(k)_{\text{known}} - \psi(k)_{\text{unknown}}]/2k \qquad (4)$$

in order to obtain a constant $\Delta r(k)$ over the whole measured k space. The estimated values of E_0 are listed in Table I.

The parameter-fitting methods[14,15] were applied to obtain detailed information about the coordination structures of the Cr ions in solutions I and II. In the parameter-fitting method, the scaling factor S_0[17] was introduced to $\chi(k)$ in eq 2, and the theoretical values of $A(k)$[18] were used. The loss of photoelectrons to the inelastic scattering process $\exp(-2r/\lambda)$ in eq 2 was neglected in the calculation for the first shell. The experimental $k^3\chi(k)$ curve was calculated by the back Fourier transform of the first peak on the $|F(r)|$ curve of each specimen. In the first step, S_0, $\phi(k)$, and σ were determined by the least-squares fitting based on the $k^3\chi(k)$ curves of the reference compounds. For this purpose, $\phi(k)$ was approximated by[19] eq 5, where q_0, q_1, q_2, and q_3 were the

$$\phi(k) = q_3/k^3 + q_2k^2 + q_1k + q_0 \qquad (5)$$

parameters to be determined. Next, the structure parameters N, r, and σ for the first shell in the solutions were determined by the least-squares method, using the estimated values of S_0 and $\phi(k)$ for the reference compounds. The least-squares calculations for the $k^3\chi(k)$ curves were carried out in the range k = 4.0–11.0 $Å^{-1}$, considering the range of the used window functions. The bond lengths in the reference compounds were taken from ref 20 and 21 for the K_2CrO_4 and Cr_2O_3 crystals, respectively, and the mean values were used.

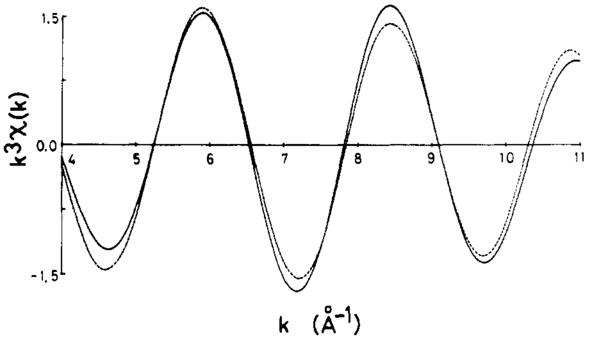

Figure 5. Final $k^3\chi(k)$ curves after least-squares parameter fitting for solution I, using S_0 and $\phi(k)$ for the K_2CrO_4 crystal: solid line, observed; broken line, calculated.

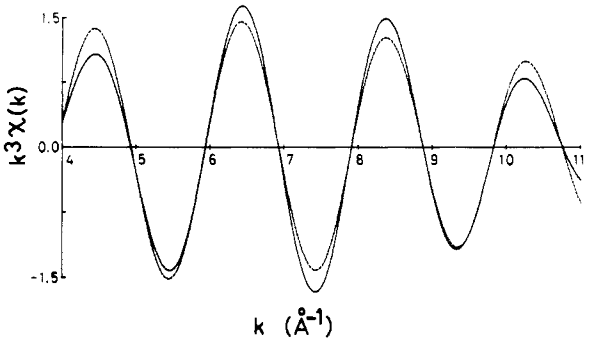

Figure 6. Final $k^3\chi(k)$ curves after least-squares parameter fitting for solution II, using S_0 and $\phi(k)$ for the Cr_2O_3 crystal: solid line, observed; broken line, calculated.

The resulting N, r, σ, and R factor are listed in Table I. Here, the R factor is defined as in eq 6. The observed and calculated

$$R = \sum||k^3\chi(k)_{\text{obsd}}| - |k^3\chi(k)_{\text{calcd}}||/\sum|k^3\chi(k)_{\text{obsd}}| \qquad (6)$$

$k^3\chi(k)$ curves are compared in Figures 5 and 6 for the nearest-neighbor Cr–O pairs in solutions I and II, respectively, showing good agreement. There is no significant difference between the bond lengths estimated on the basis of those in the K_2CrO_4 and Cr_2O_3 crystals, as is seen in Table I. The determined Cr–O bond length in solution I is close to those found in the K_2CrO_4,[20] Li_2CrO_4,[22] $(NH_4)_2CrO_4$,[23] and $PbCrO_4$[24] crystals, in which there exist isolated CrO_4 tetrahedra. The determined Cr–O bond length in solution II is close to those found in the Cr_2O_3,[21] $VCrO_4$,[25] and $SrCr_2O_4$,[26] crystals, in which there exist the CrO_6 octahedra. The coordination numbers of the Cr ions in solutions I and II were found to be 4 and 6, respectively. Therefore, it was expected that Cr(VI) ions are tetrahedrally surrounded by four O atoms in solution I and Cr(III) ions are octahedrally surrounded by six O atoms in solution II.

The coordination structures of the Cr ions in solutions I and II were examined by using the results of the EXAFS analyses together with the chemical reaction of the Cr ions with this mixed solvent. The dissolution of CrO_3 in the $HCONH_2$ + $HCOONH_4$ solvent at room temperature is represented by decomposition reaction 7 and reaction 8. The decomposition of $HCOONH_4$

---

(12) Martens, G.; Rabe, P.; Schwentner, N.; Werner, A. *Phys. Rev. B: Solid State* **1978**, *17*, 1481.

(13) Rabe, P.; Tolkiehn, G.; Werner, A. *J. Phys. C* **1979**, *12*, 1173.

(14) Ohyanagi, H.; Tsuji, K.; Hosoya, S.; Minomura, S.; Fukamachi, T. *J. Non-Cryst. Solids* **1980**, *35/36*, 555.

(15) Miyake, M.; Okuno, M.; Suzuki, T.; Marumo, F. *Nippon Kagaku Kaishi* **1982**, 905.

(16) Citrin, P. H.; Eisenberger, P.; Kincaid, B. M. *Phys. Rev. Lett.* **1976**, *36*, 1346.

(17) Stern, E. A.; Bunker, B. A.; Heald, S. M. *Phys. Rev. B: Condens. Matter* **1980**, *21*, 5521.

(18) Teo, B.-K.; Lee, P. A. *J. Am. Chem. Soc.* **1979**, *101*, 2815.

(19) Lee, P. A.; Teo, B.-K.; Simons, A. L. *J. Am. Chem. Soc.* **1977**, *99*, 3856.

(20) McGinnety, J. A. *Acta Crystallogr., Sect. B: Struct. Crystallogr. Cryst. Chem.* **1972**, *B28*, 2845.

(21) Wyckoff, R. W. G. "Crystal Structures"; Interscience: New York, 1964; Vol. 2, p 6.

(22) Brown, I. D.; Faggiani, R. *Acta Crystallogr., Sect. B: Struct. Crystallogr. Cryst. Chem.* **1975**, *B31*, 2364.

(23) Stephens, J. S.; Cruickshank, D. W. J. *Acta Crystallogr., Sect. B: Stryct. Crystallogr. Cryst. Chem.* **1970**, *B26*, 437.

(24) Quareni, S.; De Pieri, R. *Acta Crystallogr.* **1965**, *19*, 287.

(25) Wyckoff, R. W. G. "Crystal Structures"; Krieger Publishing Co.: FL, 1981; Vol. 3, p 37.

(26) Pausch, Von H.; Müller-Buschbaum, Hk. *Z. Anorg. Allg. Chem.* **1974**, *405*, 1.

$$\mathrm{HCOONH_4 \rightarrow HCONH_2 + H_2O} \tag{7}$$

$$\mathrm{CrO_3 + H_2O \rightarrow 2H^+ + CrO_4^{2-}} \tag{8}$$

into $\mathrm{HCONH_2}$ and $\mathrm{H_2O}$ was reported by Suzuki et al.;[1] i.e., the decomposition amount of $\mathrm{HCOONH_4}$ is equivalent to that of $\mathrm{CrO_3}$. As the $\mathrm{CrO_4^{2-}}$ anions are stable, it was concluded that there exist mononuclear $\mathrm{CrO_4^{2-}}$ tetrahedra with Cr–O bond lengths of 1.61 Å at the initial state of the dissolution of $\mathrm{CrO_3}$ in the $\mathrm{HCONH_2 + HCOONH_4}$ solvent.

Next, $\mathrm{HCOONH_4}$ dissociates into the $\mathrm{HCOO^-}$ and $\mathrm{NH_4^+}$ ions in a solvent with a large dielectric constant, such as $\mathrm{HCONH_2}$ (109 at 20 °C). The $\mathrm{NH_4^+}$ ion decomposes into $\mathrm{H^+}$ and $\mathrm{NH_3}$, and $\mathrm{NH_3}$ leaves the system at 90 °C (eq 9).

$$\mathrm{HCOONH_4 \rightarrow HCOO^- + H^+ + NH_3\uparrow} \tag{9}$$

When the temperature of the system is increased, Cr(VI) ions are reduced by the heated $\mathrm{HCOO^-}$ anions, as shown in eq 10–12.

$$\mathrm{HCOO^- \rightarrow {}^1/_2H_2\uparrow + CO_2\uparrow + e^-} \tag{10}$$

$$\mathrm{CrO_4^{2-} + 3e^- \rightarrow Cr^{3+} + 4O^{2-}} \tag{11}$$

$$\mathrm{O^{2-} + 2H^+ \rightarrow H_2O\uparrow} \tag{12}$$

Thus, Cr(III) ions are coordinated to six O atoms with high electron densities coming from either $\mathrm{HCOO^-}$ ions or $\mathrm{HCONH_2}$ molecules and form octahedral complexes in solution II as shown in eq 13, where $x + y = 6$.

$$\mathrm{Cr^{3+}} + x\mathrm{HCOO^-} + y\mathrm{HCONH_2} \rightarrow [\mathrm{Cr(HCOO)}_x(\mathrm{HCONH_2})_y]^{3-x} \tag{13}$$

The Cr ions were considered not to be coordinated to N atoms because, in addition to the reason mentioned above, the Cu ions, which form amine complexes more easily than the Cr ions, were found to be bonded to the O atoms in the $\mathrm{HCONH_2 + HCOONH_4}$ system by ESR spectral analyses.[1] The formation of anionic complexes of Cr(III) ions in solution II was supported by the experimental results that Cr(III) ions were removed by $\mathrm{OH^-}$-form anion-exchange resin;[27] i.e., removal ratios by $\mathrm{OH^-}$ and $\mathrm{H^+}$ resins are 95 and 3%, respectively. Only one of two O atoms in the $\mathrm{HCOO^-}$ ion is shared at the corner of the octahedron because the O···O distance within the octahedron is about 2.83 Å and that within the $\mathrm{HCOO^-}$ ion is about 2.22 Å. Therefore, x was considered to be equal to 4, 5, or 6 although it is difficult to decide the exact value of x. From the above examination, the mononuclear $[\mathrm{Cr(HCOO)}_x(\mathrm{HCONH_2})_y]^{3-x}$ ($x + y = 6$; $4 \le x \le 6$) octahedra with Cr–O bond lengths of 2.00 Å were concluded to be produced in the $\mathrm{HCONH_2 + HCOONH_4}$ system by heating reduction. The blackish corrosion-resistant chromium film produced by electrodeposition[2] is probably ascribed to the existence of $[\mathrm{Cr(HCOO)}_x(\mathrm{HCONH_2})_y]^{3-x}$ complexes in the $\mathrm{HCONH_2 +}$ $\mathrm{HCOONH_4}$ system.

Acknowledgment. This work was supported by a Grant-in-Aid for Encouragement of Research A from the Japanese Ministry of Education (No. 58750633). We thank the staff of the Photon Factory of the National Laboratory for High Energy Physics (KEK) for providing beam time. The computations were carried out on an ACOS 850 computer at the Computer Center of Yamanashi University.

Registry No. $\mathrm{CrO_4^{2-}}$, 13907-45-4; $\mathrm{CrO_3}$, 1333-82-0; $\mathrm{HCOONH_4}$, 540-69-2; $\mathrm{HCONH_2}$, 75-12-7.

---

(27) Ayuzawa, N.; Hayakawa, Y.; Suzuki, T. *Denki Kagaku oyobi Kogyo Butsuri Kagaku* **1981**, *49*, 521.

Notes

Contribution from the Departments of Chemistry,
University of Hong Kong, Hong Kong,
and The Chinese University of Hong Kong,
Shatin, New Territories, Hong Kong

High-Valent Schiff-Base Complexes of Osmium. X-ray Crystal Structure of *trans*-[$\mathrm{Os^{IV}}$(salen)(SPh)$_2$]

Chi-Ming Che,*[1a] Wing-Kin Cheng,[1a]
and Thomas C. W. Mak*[1b]

Received March 26, 1985

High-valent iron, ruthenium, and osmium metalloporphyrin complexes containing oxide ($\mathrm{O^{2-}}$), alkoxide ($\mathrm{OR^-}$), or mercaptide ($\mathrm{SR^-}$) ligands are potentially useful model systems for cytochromes or oxygenase. As part of a program to investigate the chemistry of osmoglobin,[2] we have been interested in the chemistry of osmium Schiff-base complexes because these species are expected to exhibit chemistry similar to that of the analogous porphyrin.[3] Here the synthesis and characterization of some high-valent Schiff-base complexes of osmium are described.

Experimental Section

Materials. $\mathrm{K_2[OsO_2(OH)_4]}$ and salenH$_2$ (salen = *N*,*N'*-ethylenebis(salicyclideneaminate)) were prepared as described in the literature.[4] All solvents used were of analytical grade. Triphenylphosphine (Merck 98%) and thiophenol (Aldrich 99%) were used as supplied.

***trans*-[$\mathrm{Os^{VI}}$(salen)O$_2$] (1).** $\mathrm{K_2[OsO_2(OH)_4]}$ (0.5 g) and salenH$_2$ (0.4 g) were stirred in methanol (150 mL) for 30 min. An orange-red solid gradually formed. This is filtered off, washed with a methanol/diethyl ether mixture (1:10), and dried under vacuum at room temperature; yield 85%. Anal. Calcd for $\mathrm{OsC_{16}H_{14}N_2O_4}$: C, 39.34; H, 2.86; N, 5.75. Found: C, 39.43; H, 2.62; N, 5.84. IR ν(Os=O): 840 cm^{-1}. The complex is virtually insoluble in common organic solvents.

***trans*-[$\mathrm{Os^{IV}}$(salen)(OMe)$_2$] (2a).** A methanolic suspension of **1** (0.5 g in 100 mL) and PPh$_3$ (1.4 g) was heated with stirring at 50 °C for 20 min. A deep red-brown solution was obtained, which was then filtered off and rotatory evaporated to dryness. The dry residue was dissoved in $\mathrm{CH_2Cl_2}$ and transferred to the top of a silica gel column. The PPh$_3$ was removed by eluting with $\mathrm{CH_2Cl_2}$ (300 mL), and the Os(IV) product was eluted out as a brick red band by using acetone/methanol (1:1) mixture as the eluent. Crystals of **2a** were obtained by slow diffusion of hexane into a dichloromethane solution of the crude product. Yield: ~75%. Anal. Calcd for $\mathrm{OsC_{18}H_{20}N_2O_4}$: C, 41.68; H, 3.86; N, 5.40. Found: C, 41.2; H, 3.85; N, 5.25. UV–vis spectrum in $\mathrm{CH_3CN}$, $\lambda_{\max}$/nm ($\epsilon_{\max}$/(dm^3 mol^{-1} cm^{-1})): 413 (10 500), 352 (11 900), 252 (8200).

***trans*-[$\mathrm{Os^{IV}}$(salen)(OEt)$_2$] (2b).** The complex was similarly prepared as described for **2a** except that absolute ethanol was used instead of methanol. Yield: ~68%. Anal. Calcd for $\mathrm{OsC_{20}H_{24}N_2O_4}$: C, 43.96; H, 4.39; N, 5.13. Found: C, 43.70; H, 4.10; N, 4.95. UV–vis spectrum in $\mathrm{CH_3CN}$, $\lambda_{\max}$/nm ($\epsilon_{\max}$/(dm^3 cm^{-1} mol^{-1})): 410 (17 700), 350 (15 500), 255 (15 100).

***trans*-[$\mathrm{Os^{IV}}$(salen)(SPh)$_2$] (3).** Thiophenol (5 mL) was added dropwise to a stirred dichloromethane suspension of **1** (0.5 g in 100 mL). After 15 min, a deep bluish green solution was obtained. This was evaporated off to dryness. The crude solid was washed with petroleum ether (60–80 °C) to remove excess thiophenol and purified on a silica gel column with $\mathrm{CH_2Cl_2}$ as the eluent. Blue crystalline solids of **3** were

---

(1) (a) University of Hong Kong. (b) The Chinese University of Hong Kong.

(2) Margalit, R.; Pecht, I.; Che, C.-M.; Chiang, H.-J.; Gray, H. B., "Abstracts of Papers" 185th National Meeting of the American Chemical Society, Seattle, WA, March 22, 1983; American Chemical Society: Washington, DC; INOR 42.

(3) Che, C.-M.; Poon, C. K.; Chung, W. C.; Gray, H. B. *Inorg. Chem.* **1985**, *24*, 1277.

(4) (a) Malin, J. M. *Inorg. Synth.* **1980**, *20*, 61. (b) Earnshaw, A.; King, E. A.; Larkworthy, L. F. *J. Chem. Soc. A* **1968**, 1048.

0020-1669/86/1325-0703$01.50/0